Transition densities in ^{30}Si studied by electron scattering and coupled-channel calculations of 650 MeV proton scattering

R. A. Miskimen,* A. M. Bernstein, G. Bernhardt, and C. F. Williamson
Laboratory for Nuclear Science and Department of Physics, Massachusetts Institute of Technology, Cambridge, Massachusetts 02139

B. A. Brown
Cyclotron Laboratory, Michigan State University, East Lansing, Michigan 48823

R. Alarcon
Nuclear Physics Laboratory and Department of Physics, University of Illinois, Champaign, Illinois 61820
(Received 8 October 1987)

Proton and neutron transition densities in ^{30}Si are examined by a combination of intermediate energy (e,e') and (p,p') reactions and mirror electromagnetic transition rates. This analysis is performed for the 2_1^+ and 2_2^+ states at 2.234 and 3.499 MeV in ^{30}Si. Electron scattering data are presented for these states. Shell-model calculations for the proton and neutron transition matrix elements and proton transition densities are compared with the electromagnetic results. The proton transition densities are reasonably predicted for the 2_1^+ state but are not adequately predicted for the 2_2^+ state. A microscopic coupled-channel calculation of 650 MeV (p,p') is used to test the shell-model isoscalar transition densities. Given the uncertainties present in the reaction calculation and interaction, the isoscalar density for the 2_1^+ state is found to be adequate, but the density for the 2_2^+ state is less accurate. The coupled-channel effect is shown to be important for the 2_2^+ state. This dependence increases with energy but should be taken into account for an accurate description of (p,p') reactions at all energies.

I. INTRODUCTION

Ground-state densities and transition densities are of intrinsic interest and can be used to test nuclear models. The most accurate probe of one-body densities is electron scattering.[1,2] Transitions in even-even nuclei between the 0^+ ground state and low-lying 2^+ states are mainly $C2$, and they are primarily sensitive to the protons (the smaller $E2$ matrix elements are sensitive to both proton and neutron spin currents). Hadronic probes, which are sensitive to both protons and neutrons, are needed to examine the non-spin-flip neutron transition densities. For example, the interaction for intermediate energy protons is almost isoscalar (i.e., the projectile interacts almost equally with target protons and neutrons).[3,4] This paper investigates the question of how much information can be obtained for the non-spin-flip proton and neutron transition densities, $\rho_{fi}^{p(n)}(r)$, from a combination of electromagnetic lifetimes and intermediate energy (e,e') and (p,p') reactions.

For self-conjugate nuclei ($N=Z$) the proton and neutron transition densities are approximately equal, $\rho_{fi}^{n}(r)=\rho_{fi}^{p}(r)$, and can be obtained from electron scattering in an almost model-independent way.[5] Making use of this property, a test of distorted-wave impulse approximation (DWIA) was made previously for 650 MeV protons for the self-conjugate $T=0$ nuclei ^{24}Mg, ^{28}Si, and ^{40}Ca. The results were in good agreement with experiment.[6-8] The small disagreements between DWIA prediction and data can arise from several sources, such as channel coupling,[9] medium modifications to the interaction,[10] relativistic effects,[11] and inaccuracies in the effective interaction.[4] The overall agreement between these DWIA calculations and experiment indicated that the cumulative effects of the approximation do not preclude the use of intermediate energy (p,p') for nuclear structure studies. Since non-spin-flip quantities are being examined, it is possible to use the Schrödinger equation with relativistic kinematics rather than Dirac equation phenomenology, since the differences occur primarily in the spin observables.[11]

For $N\neq Z$ nuclei $\rho_{fi}^{n}(r)$ must be known to make calculations of (p,p').[12] A purely electromagnetic technique for obtaining the magnitude of the neutron transition multipole matrix element, M_n, from mirror transition rates, has been developed previously.[13] For example, M_n for the $0^+\rightarrow 2_1^+$ transition in ^{30}Si equals M_p for the isospin analog transition in ^{30}S. It is also true that the neutron transition density in ^{30}Si equals the proton transition density in ^{30}S, though this is a much less useful constraint since the proton density in ^{30}S is unknown. The relationship between the transition matrix elements and the transition densities is given by

$$M_{p(n)}=\int_0^\infty \rho_{fi}^{p(n)}(r)r^{L+2}dr\ , \tag{1}$$

where L is the multipolarity of the transition. The radial shape of $\rho_{fi}^{n}(r)$ is not determined from the mirror method, so that a nuclear model must be utilized. However, the magnitude of $\rho_i^n(r)$ is constrained by the mirror measurement of M_n. This constraint was used previously to make predictions in DWIA for 650 MeV (p,p') to the

2_1^+ and 2_2^+ states of the $T=1$ nuclei ^{26}Mg, ^{30}Si, ^{34}S, and ^{40}Ca.[6,7] Because the radial shape of $\rho_{fi}^{n}(r)$ was not known, only the magnitude of the calculated differential cross section at the first maximum was compared to experiment. The good overall agreement between the calculated and experimental peak cross sections of these $T=1$ nuclei (at the 20% level) encouraged us to investigate the sensitivity of the (p,p') differential cross sections beyond the first maximum to the transition densities.

Ray and Hoffmann have made a model-dependent study of the sensitivity of 800 MeV (p,p') to the proton and neutron transition densities.[14] This was done for the 3^- state in ^{208}Pb at 2.61 MeV. Using a Tassie model[15] for the transition densities, they found that at the first maximum of the differential cross section there is little sensitivity to either the radius or diffuseness parameters of the Tassie model. At the first maximum, sensitivity is due primarily to the proton and neutron transition matrix elements, $M_{p(n)}$. At scattering angles beyond the first maximum of the differential cross section there is sensitivity to the radius and diffuseness parameters of the model. The sensitivity to the radius parameter is especially strong, and changes in this parameter can shift the angular positions of the minima; a larger radius shifts the minima inward and a smaller radius shifts the minima outward.

More recently, Kelly has investigated in a nearly model-independent fashion the sensitivity of medium energy (p,p') to proton and neutron transition densities.[16–18] The analysis covered proton energies from 60 to 800 MeV. He found a window of visibility between about 200 and 500 MeV where the sensitivity to nuclear structure is optimal, and nearly rivals that of (e,e'). Even at 650–800 MeV, he concluded, the sensitivity is adequate.

In this paper we will use medium energy (e,e') and (p,p') reactions and mirror matrix elements to test models for $\rho_{fi}^{p(n)}(r)$. This will be done for the ^{30}Si 2_1^+ and 2_2^+ states at 2.234 and 3.499 MeV. This nucleus was chosen for the following reasons: (1) high-momentum-transfer (e,e') data are available for these states ($0.6<q<2.1$ fm^{-1}),[19] (2) the mirror matrix elements in ^{30}S are known,[20] (3) medium energy (p,p') data are available for these states,[6–8] (4) and a shell-model calculation is available,[21] providing a model for $\rho_{fi}^{p(n)}(r)$. Our intent is to test nuclear models, not to fit neutron transition densities or matrix elements. A technique has recently been developed to fit an effective interaction to as many as nine states in a self-conjugate nucleus ($N=Z$).[16–18] The effective interaction is then applied to a nucleus where $N\neq Z$ and the neutron densities are fitted with a complete set of basis functions. This approach is not practical for the present study because of the limited (p,p') and (e,e') data sets available for ^{28}Si and ^{30}Si. The data sets are limited both in terms of the number of excited states and the angular range of the data. Also, the formalism neglects the coupled-channel effect, which we will demonstrate is important at 650–800 MeV. In this paper we report the results of a microscopic coupled-channel analysis that is, to our knowledge, the first for medium energy (p,p') that uses an interaction obtained from nucleon-nucleon scattering and transition densities from either a nuclear structure calculation or from (e,e').

In Sec. II of this paper the shell-model calculation is briefly discussed. Shell-model transition matrix elements for the 2_1^+ and 2_2^+ states of ^{30}Si are compared with matrix elements obtained using the mirror method. Electron scattering data for the 2_1^+ and 2_2^+ states are presented in Sec. III. Transition charge densities obtained from a Fourier-Bessel analysis of the (e,e') data are compared with predictions from the shell model. In Sec. IV a microscopic coupled-channel calculation of 650 MeV (p,p') is presented and compared with data. To calibrate the analysis, 650 MeV (p,p') is calculated for scattering to the ground, 2_1^+, and 4_1^+ states of ^{28}Si. This is a case where the nuclear structure is well constrained from electron scattering. In Sec. V the energy dependence of the coupled-channel effect is studied in model calculations. The coupling-strength dependence of the effect for medium energy (p,p') is also studied. Finally, in Sec. VI conclusions are drawn regarding the accuracy of the shell model and the ability of medium energy (p,p') to test its predictions.

II. SHELL-MODEL AND MIRROR MATRIX ELEMENTS

The theoretical transition densities used for comparison in this study are from the shell-model calculation of Brown, Radhi, and Wildenthal. The details of this calculation have been reported elsewhere,[21] and only a brief discussion of their results is presented here. The shell-model transition density is a sum of valence and core polarization components,

$$\rho_{sm}^{p(n)}(r)=\rho_{v}^{p(n)}(r)+\rho_{c}^{p(n)}(r)\ , \tag{2}$$

where ρ_v and ρ_c are the valence and core polarization transition densities, respectively. $\rho_v^{p(n)}(r)$ was calculated using a $0d_{5/2}-1s_{1/2}-0d_{3/2}$ shell-model space. A Tassie-model shape was postulated for the core polarization densities, and the core polarization multipole matrix elements are given by[22]

$$M_{p}^{c}=\delta^{pp}M_{p}^{v}+\delta^{pn}M_{n}^{v}\ , \tag{3a}$$

$$M_{n}^{c}=\delta^{np}M_{p}^{v}+\delta^{nn}M^{n^{v}}\ , \tag{3b}$$

where $M_{p(n)}^{v}$ and $M_{p(n)}^{c}$ are the valence and core transition multipole elements, respectively, and are related to the valence and core transition densities by Eq. (1). δ^{np}, for example, is the parameter for the polarization of core neutrons by valence protons. The average polarization values for the s-d shell, $e_p=1+\delta^{pp}=1+\delta^{nn}=1.35$ and $e_n=\delta^{np}=\delta^{pn}=0.35$, were used.[21]

In Table I the experimental values of $M_{p(n)}$ for the $0^+\rightarrow 2_1^+$, $0^+\rightarrow 2_2^+$, and $2_1^+\rightarrow 2_2^+$ transitions in ^{30}Si are listed.[20] The values of M_n come from lifetime measurements in ^{30}S and by invoking mirror symmetry so that $M_p(^{30}\text{S})=M_n(^{30}\text{Si})$. Note that the experiments measure only the square of the matrix elements, so that the absolute signs of the matrix elements are undetermined. Also shown in Table I are the shell model values of $M_{p(n)}$, which are broken down into the valence contributions. It

TABLE I. Experimental (Ref. 20) and shell-model transition matrix elements for the $0^+ \rightarrow 2_1^+$, $0^+ \rightarrow 2_2^+$, and $2_1^+ \rightarrow 2_2^+$ transitions in ^{30}Si. M_0 and M_1 are the isoscalar and isovector matrix elements. $M^v_{p(n)}$ are the valence shell-model matrix elements. The units are fm^2.

	Experiment					Shell model					
Transition	$\lvert M_p \rvert$	$\lvert M_n \rvert$	$\lvert M_0 \rvert$	$\lvert M_1 \rvert$	M_1/M_0	M_p	M_n	M^v_p	M^v_n	M_0	M_1
$0^+ \rightarrow 2_1^+$	14.3 ±0.4	20.5 ±2	34.8±2	6.2±2	0.18±0.06	−14.1	−16.0	−7.87	−9.84	−30.1	+1.90
$0^+ \rightarrow 2_2^+$	6.47±0.3	3.65±0.5	10.1±0.6	2.8±0.6	0.28±0.06	−7.89	−2.04	−5.85	+0.009	−9.93	−5.85
$2_1^+ \rightarrow 2_2^+$	16.3 ±4					+18.1	+20.0	+10.3	+12.2	+38.1	−1.90

can be seen that in the framework of this model the core polarization contributions are large, for these transitions typically 50%. It is interesting to observe that the shell model predicts the $0^+ \rightarrow 2_2^+$ transition to be nearly a pure proton transition, since M^v_n is approximately zero. Also apparent from Table I is that for $M_{p(n)}$ the agreement is slightly better between theory and experiment for the $0^+ \rightarrow 2_1^+$ transition than the $0^+ \rightarrow 2_2^+$ transition (data on the $2_1^+ \rightarrow 2_2^+$ transition are too poor to draw any conclusions). For the $0^+ \rightarrow 2_1^+$ transition the shell-model result is in good agreement with experiment for M_p, and is 22% low for M_n. For the $0^+ \rightarrow 2_2^+$ transition the shell-model result is 22% high for M_p and is 44% low for M_n.

To gauge the isovector content of the transition, the experimental proton and neutron transition matrix elements were combined into isoscalar ($M_0 = M_n + M_p$) and isovector ($M_1 = M_n - M_p$) matrix elements and listed in Table I. Here it was assumed that the transitions are predominately isoscalar, and therefore the proton and neutron transition matrix elements have the same relative sign. The isoscalar and isovector matrix elements from the shell model are also shown in Table I. In contrast to the comparison of theory and experiment for $M_{p(n)}$, the shell-model isoscalar matrix elements are in good agreement with experiment for both 2_1^+ and 2_2^+ states. The shell-model isovector matrix elements for both states, however, are in very poor agreement with experiment; theory is 70% low for the 2_1^+ state and is 110% high for the 2_2^+ state. This is believed to be a result of the large uncertainties present in the isovector effective charge, which is very sensitive to the radial wave functions used in the shell-model calculation.[23] By comparison the isoscalar effective charge is well determined.

III. ELECTRON SCATTERING TRANSITION DENSITIES

Electron scattering on natural silicon has been performed previously and the experimental details are reported elsewhere.[24] The effective momentum transfer in the experiment ranged from approximately 0.6 to 2.1 fm^{-1}. Cross sections for excited states in ^{30}Si were obtained from the (e,e') spectra,[19] and are listed in Table II. Figure 1 is a plot of the transition form factors for the 2_1^+ and 2_2^+ states of ^{30}Si. Data from this measurement and from a previous experiment at lower q_{eff} are shown.[25] Using a DWBA Fourier-Bessel analysis,[5] transition charge densities have been fitted for the 2_1^+ and 2_2^+ states using both the high and low q_{eff} data sets. It has been shown that the optimum number of Fourier-Bessel amplitudes to use in fitting is limited by the maximum momentum transfer of the data.[5] In this case $q_{max} = 2.1$ fm^{-1} and five amplitudes were fitted. The truncation error that results from limiting the number of amplitudes is not important in fitting form factors up to a value of q_{max}. However, errors will be introduced into calculations of the transition density, particularly those momentum components of the density with momentum greater than q_{max}. Typically this will effect representations of the

TABLE II. Electron scattering cross sections for scattering to the 2_1^+ and 2_2^+ states of ^{30}Si. The units are in units of mb/sr.

Energy (MeV)	Angle (deg)	q_{eff} (fm^{-1})	2_1^+ (mb/sr)	2_2^+ (mb/sr)
148.1	45.0	0.59	$7.1\pm2.7\times10^{-3}$	$2.8\pm2.0\times10^{-3}$
174.6	45.0	0.69	$4.8\pm1.2\times10^{-3}$	$1.24\pm0.82\times10^{-3}$
166.4	90.0	1.22	$1.067\pm0.063\times10^{-4}$	$4.20\pm0.34\times10^{-5}$
170.9	90.0	1.25	$8.16\pm0.47\times10^{-5}$	$3.44\pm0.24\times10^{-5}$
199.3	45.0	0.77	$3.69\pm0.48\times10^{-2}$	$1.10\pm0.37\times10^{-3}$
199.4	90.0	1.46	$1.03\pm0.25\times10^{-5}$	$8.1\pm1.5\times10^{-6}$
225.7	45.0	0.89	$3.45\pm0.52\times10^{-3}$	$7.6\pm3.0\times10^{-4}$
229.0	90.0	1.62	$8.0\pm3.8\times10^{-7}$	$1.0\pm0.33\times10^{-6}$
251.0	90.1	1.83	$1.06\pm0.21\times10^{-5}$	$3.0\pm11.0\times10^{-7}$
265.5	90.1	1.93	$3.21\pm0.48\times10^{-6}$	
279.8	90.0	2.12	$3.09\pm0.40\times10^{-6}$	$3.8\pm1.3\times10^{-7}$
293.1	90.0	2.12	$2.31\pm0.28\times10^{-6}$	$3.3\pm1.1\times10^{-7}$

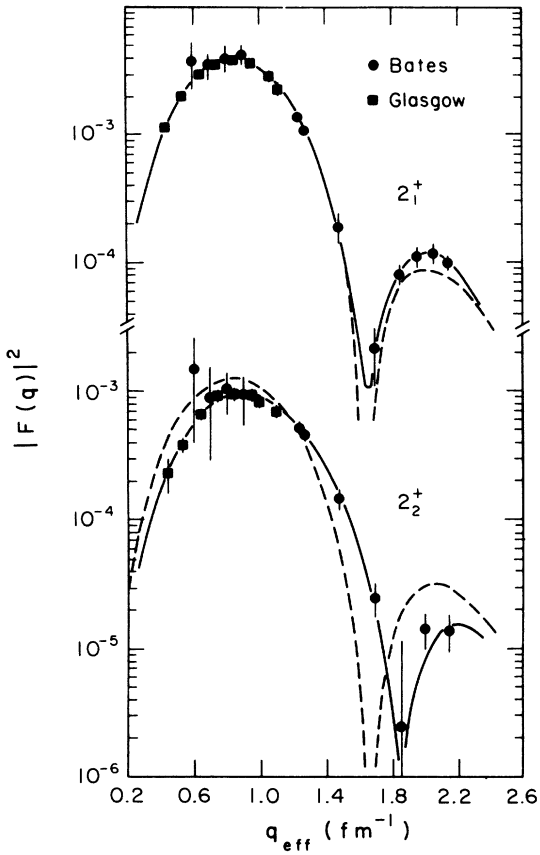

FIG. 1. (e,e') transition form factors for the ^{30}Si 2_1^+ and 2_2^+ states (upper and lower curves, respectively). q_{eff} is the effective momentum transfer (Ref. 5). The data represented by circles are data reported in this paper. The data represented by squares are from a previous experiment (Ref. 25). The solid curves are fitted form factors resulting from the DWBA model-independent analysis. The dashed curves are the shell-model transition form factors.

transition density in the nuclear interior, in this case within approximately 1 fm. However, this error will not be important in considerations of medium energy proton scattering since the proton is predominately sensitive to the nuclear surface. The form factors resulting from the fit are shown as the solid curves in Fig. 1. The shapes of the two expermental transition form factors are similar, the major difference being that the minimum for the 2_2^+ state is shifted outward by 0.2 fm^{-1} relative to the 2_1^+ minimum. Table III lists the fitted Fourier-Bessel amplitudes resulting from the analysis.

Figure 1 compares the shell-model electron scattering form factor with data for the 2_1^+ state. Agreement with data at low q_{eff} and in the position of the minimum is very good. Only at high q_{eff} do theory and data disagree. Figure 2(a) shows the shell-model and experimental transition charge densities for the 2_1^+ state. This is the same comparison as in Fig. 1, but now as a function of r instead of q_{eff}. The agreement between shell-model density and experimental density is good in both the surface and peak regions, differing moderately only in the nuclear interior.

Figure 1 also compares the shell-model and experimental electron scattering form factors for the 2_2^+ state. The agreement seen in the 2_2^+ state is relatively poor, especially when compared to the good agreement found in the 2_1^+ state. Theory disagrees with data over the entire range of q measured from low to high q_{eff} and in the position of the minimum. Figure 2(b) compares the transition charge densities for the 2_2^+ state. As anticipated from the form factor comparison, the shell-model transition density is in poor agreement with data in both the nuclear surface and interior regions. The 2_2^+ state is especially interesting in that the valence neutron matrix element M_n^v is almost zero (see Table I). In the framework of the shell model this means that $\rho_{fi}^p(r)$ for this state is dominated by the valence contribution, and the disagreement with experiment both in magnitude and shape is therefore primarily in the shell-model (valence) calculation.

IV. MICROSCOPIC COUPLED-CHANNEL CALCULATION FOR (p,p')

Coupled-channel calculations of 650 MeV (p,p') were made for scattering to the ground, 2_1^+, and 2_2^+ states of ^{30}Si. They were made using the program ECIS79,[26] with elastic and transition potentials input externally. The potentials used as external inputs to ECIS79 were generated using the program ALLWRLD,[27] which folds a nucleon-nucleon interaction with ground-state or transition densities. The interaction used is the free nucleon-nucleon interaction of Love and Franey.[4] The elastic potential is a first-order optical potential that includes central and spin-orbit terms, and is calculated from the Love-Franey interaction and the ground-state proton[25] and neutron densities (assuming $\rho_{gs}^n = \rho_{gs}^p$).

The transition potentials used for the coupled-channel analysis are calculated using the shell-model isoscalar and isovector transition densities; i.e., both the shell-model proton and neutron transition densities are used. Despite evidence from the mirror matrix elements that the isovector predictions of the shell model are somewhat unreliable, there is no disadvantage in including the shell-model isovector density in these calculations. This is be-

TABLE III. Fourier-Bessel amplitudes (Ref. 5) for the 2_1^+ and 2_2^+ transition charge densities in ^{30}Si. R is the cut-off radius for the transition density. The $B(E2)$s resulting from the fitting procedure and the actual experimental values (Ref. 20) are listed for comparison.

State	R (fm)	A_1	A_2	A_3	A_4	A_5	Fitted $B(E2)$	Expt. $B(E2)$
2_1^+	7.0	+0.019 13	+0.028 48	+0.004 52	−0.010 20	−0.005 12	198.0±7.0	203.0±12
2_2^+	7.0	+0.009 13	+0.015 96	+0.007 05	−0.002 86	−0.002 96	41.4±2.6	41.8±3.9

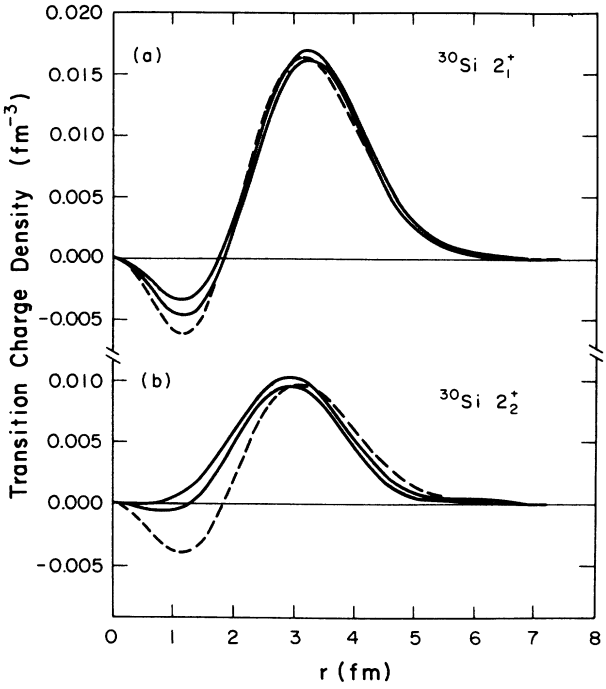

FIG. 2. Transition charge densities for (a) the ^{30}Si 2_1^+ state and (b) the ^{30}Si 2_2^+ state. The solid curves indicate the error bands of the experimental transition densities. The dashed curves are the shell-model densities.

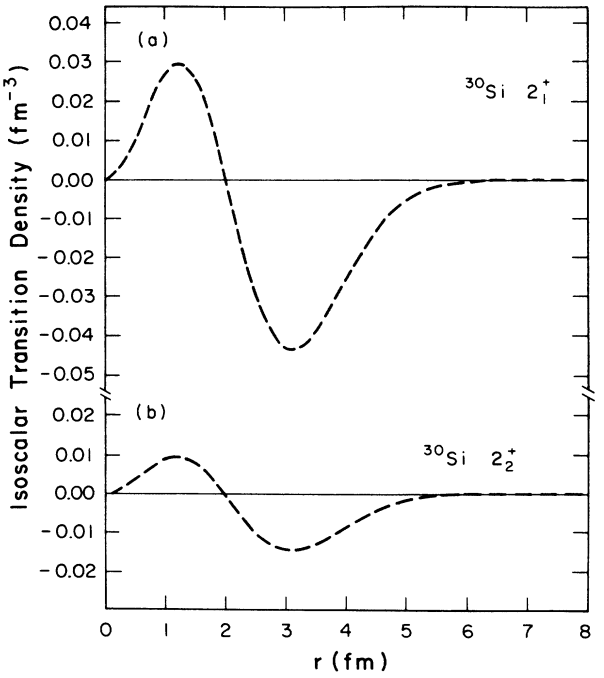

FIG. 3. Shell-model isoscalar transition densities for (a) the ^{30}Si 2_1^+ state and (b) the ^{30}Si 2_2^+ state.

cause the interaction for medium energy protons is almost isoscalar, and the (p,p') calculations are generally insensitive to inaccuracies in the isovector densities.[8] Therefore, medium energy (p,p') can only test isoscalar predictions of the shell model. The shell model isoscalar densities used in this calculation for the $0^+ \rightarrow 2_1^+$ and $0^+ \rightarrow 2_2^+$ transitions are shown in Figs. 3(a) and (b). Although the interaction includes central, spin-orbit, and tensor terms, only the central and spin-orbit terms are used in calculating the transition potentials, since it is assumed all transitions are purely longitudinal with multipolarity $L=2$.

In coupling the ground, 2_1^+, and 2_2^+ states together five transition potentials are required (assuming only longitudinal transitions with multipolarity $L=2$). Three of these are for the off-diagonal transitions $0^+ \rightarrow 2_1^+$, $0^+ \rightarrow 2_2^+$, and $2_1^+ \rightarrow 2_2^+$, and two are for the diagonal transitions $2_1^+ \rightarrow 2_1^+$ and $2_2^+ \rightarrow 2_2^+$. The off-diagonal transition potentials are generated from the interaction and the shell-model transition densities. The sensitivity of the calculation to the diagonal transition potentials was investigated using the rotational model, because of its simplicity. In the rotational model the ratio of diagonal to off-diagonal matrix elements is given exactly by[28]

$$\frac{M(2^+ \rightarrow 2^+)}{M(0^+ \rightarrow 2^+)} = -\sqrt{\tfrac{10}{7}} , \tag{4}$$

so that the diagonal matrix element is actually larger than the off-diagonal matrix element in this case. In contrast, the shell model predicts the diagonal matrix elements are only approximately 20% of the off-diagonal matrix elements. Coupled-channel calculations were made using the rotational model estimate for the diagonal matrix elements and assuming a Tassie model for the shape of the transition densities. The results show little sensitivity to the diagonal coupling, and henceforth the diagonal coupling will be neglected. Therefore, with this approximation there are a total of three transition potentials coupling three states.

In DWIA the (p,p') cross section is proportional to the square of a hadronic matrix element, which in collective model DWBA is the usual β parameter.[3] Thus in impulse approximation the result is independent of the absolute signs of the matrix elements. For example, the impulse approximation result is the same if $M_p \rightarrow -M_p$ and $M_n \rightarrow -M_n$. The relative signs of the matrix elements are important, because if M_p and M_n have opposite signs, the transition is predominately isovector.[8] However, in coupled-channel calculations the absolute sign of the matrix elements is important. This is because there is now the possibility of one-step processes interfering with two-step processes. An example of this is shown in Fig. 4(a). Excitation to the 2_2^+ state can proceed directly from the ground state in a one-step process, or through a two-step process that goes through the intermediate 2_2^+ state.

Given three matrix elements coupling three states, there are eight different combinations of absolute sign. Starting with the coupled equations of Tamura,[9] it can be shown that for this situation there are only two unique solutions of the equations. Different combinations of sign only change the phase of the wave functions without affecting cross sections. This result has also been verified with actual calculations with ECIS79. Compared to the

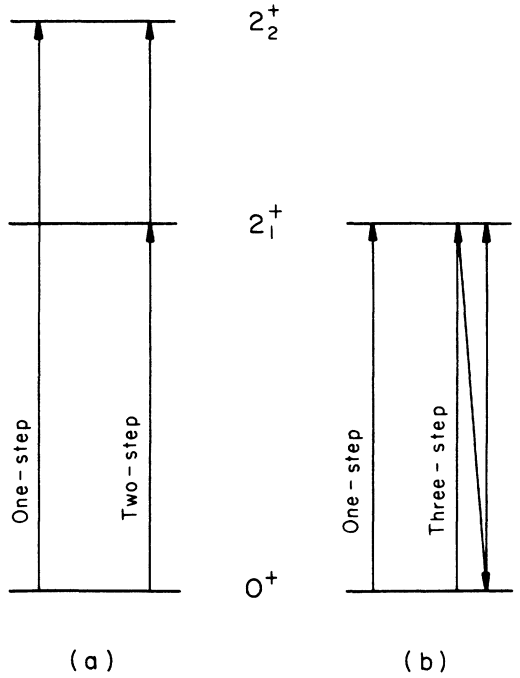

FIG. 4. Interference effects in coupled-channel calculations. (a) The interference of one-step with two-step transition amplitudes when three states are coupled. (b) The interference of one-step with three-step transition amplitudes when two states are coupled.

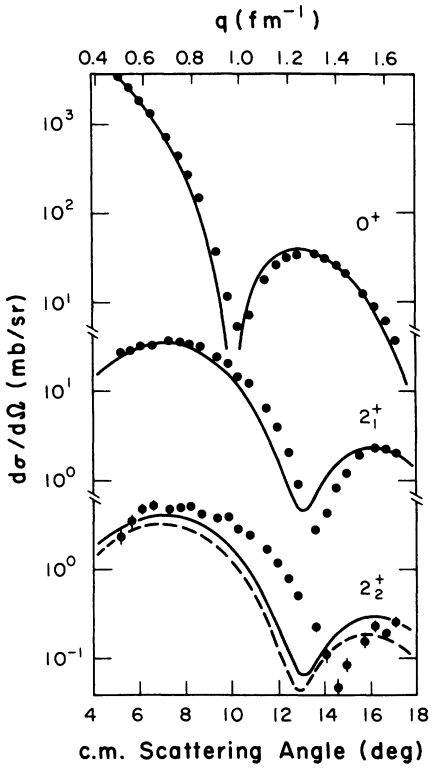

FIG. 5. Coupled-channel calculations and data for 650 MeV (p,p') to the ground, 2_1^+, and 2_2^+ states of ^{30}Si. The top ordinate is center of mass momentum transfer (fm^{-1}); the bottom is center of mass scattering angle (degrees). The shell-model transition densities are used. For the 2_2^+ state the solid line is for constructive interference of the one-step and two-step transition amplitudes, the dashed line for destructive interference. The shell-model matrix elements predict destructive interference.

impulse approximation these solutions correspond to constructive and destructive interference of the one-step amplitude with the two-step amplitude. The shell model makes a definite prediction concerning the absolute signs of these matrix elements, so there is only one solution. However, in this paper both solutions of the coupled equations will be presented, because we hope to test not only the magnitudes of the transition matrices and densities but also the absolute signs of the matrix elements and the sensitivity of medium energy (p,p') to the coupled-channel effect.

Figure 5 compares the results with experiment. Proton scattering at 650 MeV on ^{30}Si has been described previously[8] and the data resulting from the analysis are shown here for comparison with the calculations. As was found in the comparison of transition form factors, the experimental (p,p') angular distributions for the 2_1^+ and 2_2^+ states have similar shapes, the major difference being an outward shift of the 2_2^+ minimum by 0.1 fm^{-1} relative to the 2_1^+ minimum. The coupled-channel calculation has been performed for both solutions of the coupled equations. However, only for the 2_2^+ state is the difference between the two calculations significant. For elastic scattering the agreement of calculation and experiment is good, and only in the region of the minimum is agreement poor. Here the predicted minimum is deeper and at a smaller momentum transfer than the data, by approximately 0.05 fm^{-1}. The agreement between theory and experiment for the 2_1^+ state is also good, particularly at the first and second maxima. The minimum has the correct depth; however, the predicted position is again at too small a momentum transfer by approximately 0.05 fm^{-1}. Agreement for the 2_2^+ state is not as good as either the ground or 2_1^+ states. There is better agreement with data at the first and second maxima for the case of constructive interference than for the case of destructive interference. The shell model, however, using the absolute signs of Table I, actually predicts destructive interference. The minimum has the correct depth, although its predicted position is off by the largest amount; it is approximately 0.15 fm^{-1} too small.

To calibrate the coupled-channel analysis and the interaction, a calculation was made of 650 MeV (p,p') scattering to the ground, 2_1^+, and 4_1^+ states of ^{28}Si. This is a particularly good test case because uncertainties in the nuclear structure can be minimized. Electron scattering on ^{28}Si has been performed previously,[24] and a Fourier-Bessel analysis for the transition charge densities was made.[7] Because $Z=N$ for ^{28}Si, it is a good approximation to assume the proton and neutron transition densities are equivalent. A Tassie model was assumed for the $2_1^+ \rightarrow 4_1^+$ transition density, with a transition matrix element given by the electromagnetic decay rate. Figure 6

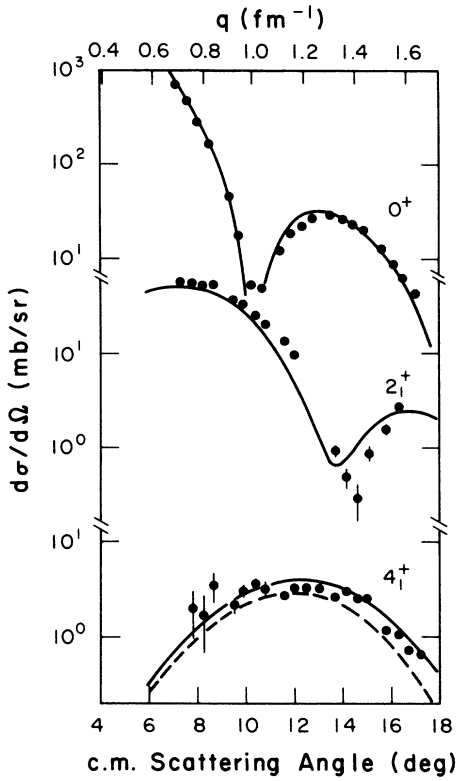

FIG. 6. Coupled-channel calculations and data (Ref. 6) for 650 MeV (p,p') to the ground, 2_1^+, and 4_1^+ states of ^{28}Si. The top ordinate is center of mass momentum transfer (fm^{-1}); the bottom is center of mass scattering angle (degrees). The proton and neutron transition densities are from (e,e') and are assumed equal. For the 4_1^+ state the solid line is for constructive interference of the one-step and two-step transition amplitudes, the dashed line for destructive interference.

compares the results with data[6] for these states. The agreement with data for the ground and 2_1^+ states of ^{28}Si is very similar to that seen for the ground and 2_1^+ states of ^{30}Si. This implies that discrepancies seen in the ground and 2_1^+ states are due to either the reaction calculation or the interaction being used. To improve agreement with data it would be necessary to use an effective interaction in the analysis, where the interaction is fitted to the data. Finally, for the 4_1^+ state, both calculations describe the data reasonably well, though it is unclear which gives better agreement.

Returning to Fig. 5 and the results for ^{30}Si, it is clear from the discussion of ^{28}Si that the agreement for the ground and 2_1^+ states of ^{30}Si is as good as expected, given the accuracy of the coupled-channel calculation. However, the agreement with data for the ^{30}Si 2_2^+ state is worse than the 2_1^+ state of either ^{30}Si or ^{28}Si. In this case the analysis does have sufficient accuracy to show that the ^{30}Si 2_2^+ transition density is not accurate. The outward shift of the minimum relative to the other 2^+ states could indicate an inward shift of the transition radius from that predicted by the shell model, a behavior that has been demonstrated in previous studies.[14] This is a model-dependent statement, but it is supported by an examination of the proton and isoscalar transition radii for these states. The isoscalar transition radius is defined by

$$\langle r^2\rangle_{fi}^0 = \frac{\int_0^\infty \rho_{fi}^0(r) r^{L+4} dr}{\int_0^\infty \rho_{fi}^0(r) r^{L+2} dr} , \tag{5}$$

where $\rho_{fi}^0(r)$ is the isoscalar density. For the ^{30}Si 2_1^+ and 2_2^+ states the isoscalar transition radii predicted by the shell model are nearly equal, 4.13 and 4.14 fm, respectively. This is an important factor in recognizing why the coupled-channel calculation predicts the same minimum position for the 2_1^+ and 2_2^+ states, while experimentally they are shifted relative to each other by 0.1 fm^{-1}. The measured proton transition radii for the 2_1^+ and 2_2^+ states are slightly different, 4.07±0.03 and 3.90±0.08 fm, respectively. Evidence for this can be seen in the electron scattering form factors, where the minimum for the 2_2^+ state is shifted outward relative to the minimum of the 2_1^+ state by 0.2 fm^{-1}. The shifts between the 2_1^+ and 2_2^+ states for both the electron and proton scattering are quite similar. This emphasizes the fact that both the proton and isoscalar transition radii are larger for the 2_1^+ state than for the 2_2^+ state.

V. ENERGY AND COUPLING DEPENDENCE OF THE COUPLED-CHANNEL EFFECT FOR (p,p')

Calculations were made to study the energy dependence of the coupled-channel effect. For example, it is generally assumed that the effect is weaker at 150–300 MeV than at 650–800 MeV. For this model study (p,p') cross sections were generated for scattering to the ground, 2_1^+, and 2_2^+ states of ^{30}Si. The energy-dependent nucleon-nucleon interaction of Love and Franey was used at proton energies of 140, 325, 515, 650, and 800 MeV. Transition densities and transition matrix elements were chosen as in Sec. IV, and cases of constructive and destructive interference were both considered, as before. For purposes of comparison, the impulse approximation result was also calculated. This was accomplished by turning off channel coupling within the ECIS79 code.

Figure 7 is a plot of the results for the 2_2^+ state (the coupled-channel effect on the 0^+ and 2_1^+ states is very small). The figure shows the percent deviation from the impulse approximation as a function of energy. This is evaluated at the peak of the first maximum of the differential cross section. Because the energy changes in this figure, the angle of the peak cross section is also changing. It varies from 15.6° in the center of mass at 140 MeV to 6.2° at 800 MeV. For constructive interference the effect at the peak of the differential cross section increases the cross section over the impulse approximation result by approximately +8% at 140 MeV to +14% at 800 MeV. For destructive interference the effect decreases the cross section below the impulse result by −7% at 140 MeV to −11% at 800 MeV. The results of this study agree with the assumption that the coupled-channel effect is weaker at 150–300 MeV than at 650–800 MeV. Nevertheless it is clearly important to take the effect into account for all energies if accurate nu-

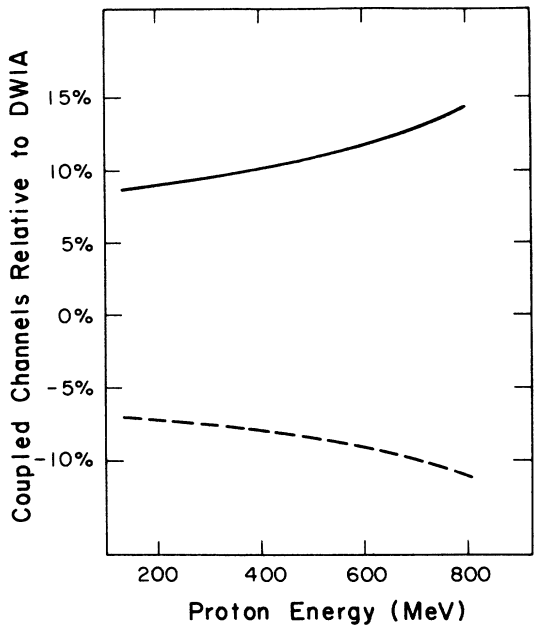

FIG. 7. Energy dependence of the coupled-channel effect for medium energy (p,p'). The percent deviation from impulse approximation at the peak of the first maximum of the ^{30}Si 2_2^+ state is plotted as a function of proton energy. The two solutions of the coupled equations are shown, corresponding to constructive and destructive interference.

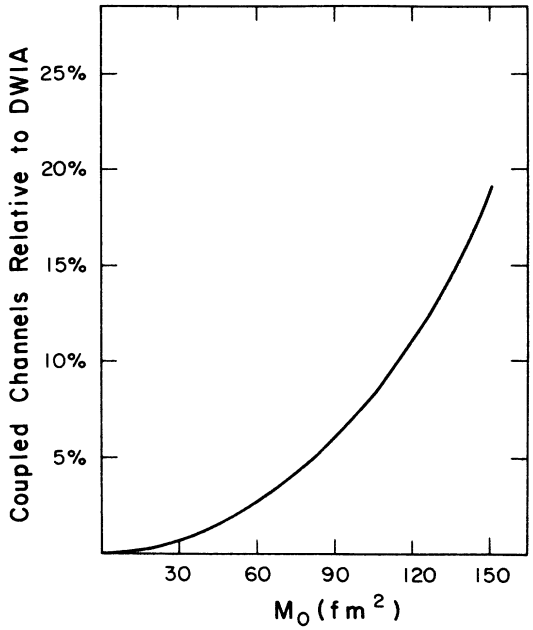

FIG. 8. Coupling strength dependence of the coupled-channel effect for 650 MeV (p,p'). Only the ^{30}Si ground and 2_1^+ states are coupled. The percent deviation from impulse approximation at the peak of the first maximum of the ^{30}Si 2_1^+ state is plotted as a function of the isoscalar matrix element. The actual experimental value of M_0 is 34.8 fm^2.

clear structure information for the weakly excited states is to be obtained. Current practice is to neglect this effect.

The coupling strength dependence of the effect can also be studied. For this model study only the ground and 2_1^+ states of ^{30}Si were coupled. Starting from the coupled equations of Tamura, it can be shown that, in this case, there is only one solution of the equations, and that it is independent of the absolute signs of the transition matrix elements. This was verified with actual calculations using ECIS79. Cross sections for 650 MeV (p,p') were then generated as a function of the transition matrix elements coupling the ground and 2_1^+ states, where the transition density shapes were held fixed.

Figure 8 is a plot of the cross section for the 2_1^+ state at the peak of the first maximum of the differential cross section. It is shown as a percent deviation from the impulse approximation. This is plotted versus the magnitude of the isoscalar transition matrix element (the isovector matrix element is also scaled with the isoscalar matrix element, though its effect on the cross section is very small). Note that the coupled-channel effect increases the cross section at the peak of the first maximum over the impulse approximation value. This can be understood as constructive interference of one-step and three-step transition amplitudes. Figure 4(b) shows how this can occur. Excitation to the 2_1^+ state can occur directly from the ground state in a one-step process. It can also occur by a three-step process where excitation to the 2_1^+ state is followed by deexcitation to the ground state, followed by excitation to the 2_1^+ state. Because only two states are coupled, there is no two-step amplitude in this case.

It is interesting to observe that this is the opposite effect of that seen in very low energy nucleon-nucleus scattering ($E_N < 50$ MeV), where the coupled-channel effect decreases the cross section.[29] The difference between low and medium energies can be understood by noting the different nature of the transition potentials in these two energy regimes. Among other factors, the transition amplitude varies as the product of the transition potentials. At low energy the transition potentials are predominately real, and at medium energy they are predominately imaginary. Therefore, one-step and three-step transition amplitudes calculated from predominately real potentials will interfere differently than if they were calculated from predominately imaginary potentials. This explains why the interference effect differs, though it does not predict the energy at which the interference is constructive or destructive.

VI. SUMMARY AND CONCLUSIONS

Medium energy (e,e') and (p,p') reactions and mirror electromagnetic matrix elements have been used to test the predictions of a shell-model calculation for the 2_1^+ and 2_2^+ states of ^{30}Si. Comparison of theory and experiment for $M_{p(n)}$ shows better agreement for the 2_1^+ than the 2_2^+ state. The shell-model isoscalar matrix elements, however, are in good agreement with experiment for both

states. The shell-model isovector matrix elements are not in agreement with either transition. Electron scattering data for the 2_1^+ and 2_2^+ states of ^{30}Si are reported. The transition charge densities of these states were determined by a Fourier-Bessel analysis. The experimental and shell-model transition form factors and charge densities were compared, resulting in good agreement for the 2_1^+ state and poor agreement for the 2_2^+ state. To test the shell-model isoscalar density, microscopic coupled-channel calculations of 650 MeV (p,p') were made for scattering to the ground, 2_1^+, and 2_2^+ states of ^{30}Si. The analysis was calibrated by carrying out a similar calculation for the ground, 2_1^+, and 4_1^+ states of ^{28}Si, cases where the transition densities are constrained by (e,e'). Comparison of data with calculation shows that the isoscalar density for the ^{30}Si 2_1^+ state is adequate. Agreement for the ^{30}Si 2_2^+ state is worse, indicating the transition radius for the shell-model isoscalar density is too large. The energy dependence of the coupled-channel effect was studied in model calculations which showed that the effect is important for the 2_2^+ state and increases as the energy increases.

In conclusion, shell-model predictions for the ^{30}Si 2_1^+ state have been shown to be accurate. Those for the ^{30}Si 2_2^+ state have been shown to be less accurate. Medium energy (p,p') can be reasonably used to test isoscalar predictions of the shell model. We have shown that the coupled-channel effect is an important consideration for nuclear structure investigations that utilize medium energy (p,p') reactions. Work in progress will extend this calculation to include the coupling to giant multipole resonances. Inelastic photon scattering has already shown that the coupling of low-lying 2^+ states to the giant dipole resonance is small, typically less than 1% of the coupling to the ground state for a heavy nucleus.[30] Much less is known about the coupling of the isoscalar giant quadrupole resonance to low-lying 2^+ states. Finally, it is desirable that an effective interaction, and a self-consistent procedure for finding such an interaction, be incorporated into the microscopic coupled-channel calculation to improve the quality of agreement with data.

ACKNOWLEDGMENTS

The authors wish to acknowledge and thank V. R. Brown and J. J. Kelly for many useful suggestions and comments. This work was supported by the U.S. Department of Energy under Contract Nos. DE-AC02-76ER03069 and DE-AC02-76ER02853.A013, and by the National Science Foundation under Contract Nos. PHY-83-12245 and PHY-86-10493.

*Present address: Department of Physics and Astronomy, University of Massachusetts, Amherst, MA 01003.

[1]T. DeForest, Jr. and J. D. Walecka, Adv. Phys. **15**, 1 (1966); T. W. Donnelly and J. D. Walecka, Ann. Rev. Nucl. Sci. **25**, 329 (1975).

[2]J. Heisenberg and H. P. Blok, Ann. Prev. Nucl. Part. Sci. **33**, 569 (1983).

[3]A. M. Bernstein, V. R. Brown, and V. A. Madsen, Phys. Lett. **103B**, 255 (1981); **106B**, 259 (1981).

[4]W. G. Love and M. A. Franey, Phys. Rev. C **31**, 488 (1985).

[5]J. Heisenberg, in *Advances in Nuclear Physics,* edited by J. W. Negele and E. Vogt (Plenum, New York, 1982), Vol. 13.

[6]R. A. Miskimen *et al.*, Phys. Lett. **131B**, 26 (1983).

[7]R. A. Miskimen, Ph.D. thesis, Massachusetts Institute of Technology, 1983 (unpublished).

[8]A. M. Bernstein *et al.*, Phys. Rev. Lett. **49**, 451 (1982).

[9]T. Tamura, Rev. Mod. Phys. **37**, 679 (1965).

[10]J. J. Kelly *et al.*, Phys. Rev. Lett. **45**, 2012 (1980).

[11]J. A. McNeil, J. R. Shepard, and S. J. Wallace, Phys. Rev. Lett. **50**, 1439 (1983).

[12]A. Chaumeaux, V. Layly, and R. Schaeffer, Ann. Phys. **116**, 247 (1978).

[13]A. M. Bernstein, V. R. Brown, and V. A. Madsen, Phys. Rev. Lett. **42**, 425 (1979).

[14]L. Ray and G. W. Hoffmann, Phys. Rev. C **27**, 2133 (1983).

[15]L. J. Tassie, Austral. J. Phys. **9**, 407 (1956).

[16]J. J. Kelly, in *Advanced Methods in the Evaluation of Nuclear Scattering Data,* Vol. 236 of *Lecture Notes in Physics,* edited by H. J. Krappe and R. Lipperheide (Springer-Verlag, Berlin, 1985), p. 335.

[17]J. J. Kelly *et al.*, Phys. Lett. **169B**, 157 (1986).

[18]J. J. Kelly, Phys. Rev. C (to be published).

[19]G. Bernhardt, M.S. thesis, Massachusetts Institute of Technology, 1983 (unpublished).

[20]T. K. Alexander *et al.*, Phys. Rev. Lett. **49**, 438 (1982), and references contained therein.

[21]B. A. Brown, R. Radhi, and B. H. Wildenthal, Phys. Rep. **101**, 313 (1983).

[22]V. R. Brown and V. A. Madsen, Phys. Rev. C **11**, 1298 (1975).

[23]B. A. Brown, International Nuclear Physics Conference, Harrogate, U.K., 1986 (unpublished).

[24]K. E. Whitner, C. F. Williamson, B. E. Norum, and S. Kowalski, Phys. Rev. C **22**, 374 (1980).

[25]S. W. Brain *et al.*, J. Phys. G **3**, 821 (1977).

[26]J. Raynal, Code ECIS79, Saclay (unpublished); IAEA Report SMR-918, 1972, p. 281.

[27]J. A. Carr, J. J. Kelly, and F. Petrovich, private communication.

[28]J. de Boer and J. Eichler, in *Advances in Nuclear Physics,* edited by Baranger-Vogt (Plenum, New York, 1968), Vol. 1.

[29]F. Perey and G. R. Satchler, Phys. Lett. **5**, 212 (1963).

[30]A. M. Nathan, P. L. Cole, P. T. Debevec, S. D. Hoblit, S. F. LeBrun, and D. H. Wright, Phys. Rev. C **34**, 480 (1986).